HI velocity fields and the shapes of dark matter halos

Schoenmakers, R. H. M.

Published in:
Dark and Visible Matter in Galaxies

HI velocity fields and the shapes of dark matter halos

R.H.M. Schoenmakers

Kapteyn Astronomical Institute, P.O. Box 800, 9700 AV, Groningen, The Netherlands.

Abstract. I report on a new method for measuring deviations from axisymmetry in the velocity fields of gas disks. The method is an extension of the method that Franx, van Gorkom and de Zeeuw developed for a single orbit gas ring. The measurement is based upon a higher order harmonic expansion of the full velocity field. Epicyclic theory is used to calculate the effects of a perturbation in the potential on these harmonic terms. It is shown how the s_1 and s_3 harmonics can be used to measure $\epsilon_R \sin(2\phi_{obs})$, where ϵ_R is the elongation of the potential and ϕ_{obs} is an (unknown) viewing angle. The advantage of this method over previous attempts to derive the elongation of dark matter halos is that, by using HI, we can probe the potential at radii beyond the stellar disk, into the regime where the dark matter is thought to be the dominant dynamical component.

As a demonstration, I applied this method to HI velocity fields of two spiral galaxies, NGC 2403 and NGC 3198. NGC 3198 shows a very small $\epsilon_R \sin(2\phi_{obs})$, which suggests that the galaxy is very nearly axisymmetric. NGC 2403 shows a larger $\epsilon_R \sin(2\phi_{obs})$, varying in a systematic way between 0 and 0.1 and is probably influenced by spiral arms. The current data suggests that spiral galaxies are close to axisymmetry, but a larger sample is needed to quantify this statement.

1. Introduction

It is generally accepted that disk galaxies have massive dark halos, but little is known about the shape of the dark matter halos. Dark halos were generally modeled as being spherical until Binney (1978) argued that the natural shape of dark halos is triaxial. If halos are indeed triaxial, the disk of the galaxy will reside in one of the principal planes of the dark halo. In a triaxial halo the axes obey the relation $a > b > c$. I will assume that the disks of spiral galaxies lie within the a, b plane.

Triaxial dark matter halos occur naturally in cosmological N-body simulations of structure formation in the universe (Katz & Gunn 1991, Dubinski & Carlberg 1991, Dubinski 1994), but the exact distribution of the halo shapes is as yet uncertain. Especially the inclusion of baryons in the simulations tends to make the halos more oblate (Dubinski 1994). So the observed distribution of the shapes of dark matter halos will be a powerful constraint on scenarios of galaxy formation and subsequent evolution.

Measuring the shapes of dark halos can be split into two parts: measurement of the ratio c/a, i.e. the flattening perpendicular to the plane of the disk, and measurement of the intermediate to major axis ratio b/a, i.e. the elongation in the plane of the disk. The axis ratio c/a can be measured using, for instance, polar ring galaxies (e.g. Whitmore, McElroy & Schweizer 1987, Sackett & Sparke 1990, Sackett *et al* 1994), kinematics of halo stars of the Milky Way (van der Marel 1991) or the flaring of HI-disks (Olling, these proceedings, Sicking 1996). All these measurements seem to indicate that $c/a < 1$, in other words, a spherical halo is excluded by these measurements.

The elongation of the dark halo (b/a) is a similarly uncertain parameter. Attempts to measure this quantity include studies of the inclination distributions of large samples of spiral galaxies and fitting models with different elongations to them (Lambas 1992, Binney & de Vaucouleurs 1981, Fasano *et al* 1992), detailed observations of the old stellar disks of spiral galaxies (Rix & Zaritsky 1995), kinematics of the milky way (Kuijken & Tremaine 1994) and the scatter in the Tully–Fisher relation (Franx & de Zeeuw 1992). All these measurements indicate that $b/a \sim 0.9$.

The only direct measurement of the elongation of the potential of a disk galaxy so far is of the S0 galaxy IC 2006 (Franx, van Gorkom & de Zeeuw 1994, hereafter FvGdZ), which contains a large HI ring in the plane of the disk. Using information on both the kinematics and the geometry of the ring, FvGdZ were able to measure the elongation of the potential at the location of the ring. The measured elongation was consistent with zero. The method used by FvGdZ was based on the assumption that one could use epicycle theory to predict the geometry and velocity field of the ring in a mildly perturbed potential. If the external potential is elongated, the velocity variation along the ring will not be precisely sinusoidal, but higher harmonic terms will be superimposed on it. Making a harmonic expansion of the velocity field of the ring and interpreting the measured harmonics within the framework of epicycle theory, given the ring geometry, the elongation of the potential at the position of the ring can be found.

I have extended the FvGdZ formalism for measuring the elongation of the potential of a single orbit gas ring to the case of a slightly non-axisymmetric gas disk, which may contain spiral-like perturbations. This analysis assumes a stationary perturbation and closed stable orbits. Therefore, applicability to non-linear phenomena like spiral arms is limited. But a small global elongation of the overall potential, as is the case with a triaxial dark matter halo, can be analysed with this method. The advantage of this method over previous attempts to derive the elongation of dark matter halos is that, by using HI, we can probe the potential at radii beyond the stellar disk, into the regime where the dark matter is thought to be the dominant dynamical component.

2.   Results from perturbation theory

Suppose the (cold) HI-disk resides in a potential

$$V(R, \phi) = V_0(R) + V_m(R) \cos(m\phi + \varphi_m(R)), \qquad (1)$$

where R and ϕ are polar coordinates in a frame that rotates with the perturbation, at a pattern speed $\Omega_{m,p}$. Here, $V_0(R)$ is the unperturbed potential, $V_m(R)$

the amplitude of the perturbation and $\varphi_m(R)$ its phase. The perturbation is assumed to be stationary. One can calculate the possible closed loop orbits of the gas in this potential (analogous to Binney & Tremaine, 1987, p. 146). Subsequently one can determine the velocity field generated by these orbits. Now assume that this velocity field is observed under viewing angles (ϕ_{obs}, i), where ϕ_{obs} is the angle between the line where $\phi = 0$ and the projection of the line-of-sight onto the plane of the disk and i is the inclination of the disk. If one then introduces the azimuthal angle $\psi = \phi - \phi_{obs} + \pi/2$ (the angle in the plane of the disk that is zero on the line of nodes), it is possible to show that the velocity field projected on the sky (hereafter "line-of-sight velocity field" or "l.o.s. velocity field") has the following form (express the line-of-sight velocity as a Fourier expansion $v_{los} = \sum_n c_n \cos n\psi + s_n \sin n\psi$):

$$v_{los} = v_* \left[c_1 \cos\psi + s_{m-1} \sin(m-1)\psi + c_{m-1}\cos(m-1)\psi \right.$$
$$\left. + s_{m+1}\sin(m+1)\psi + c_{m+1}\cos(m+1)\psi \right], \qquad (2)$$

with $v_* = v_c \sin i$ (v_c is the circular velocity) and coefficients c_x, s_x that depend on m, ϕ_{obs}, $\varphi(R)$, $V_0(R)$, $V_m(R)$ and $\Omega_{m,p}$. Now the measurable parameters (v_*, c_x, s_x) are expressed in terms of internal parameters for a potential perturbed by a single Fourier term.

From equation (2) we can conclude that *if the potential has a perturbation of Fourier number m, the l.o.s. velocity field contains $m-1$ and $m+1$ Fourier terms.* Qualitatively, this conclusion was also inferred by Canzian (1993).

In order to measure the harmonic terms in the l.o.s. velocity field, we first fit a set of tilted-rings to the l.o.s. velocity field using standard tilted-ring fitting routines. Then the velocity along each ring is decomposed into its harmonics. In general, one does not a priori know the inclination i, position angle Γ and centre (x_0, y_0) of a galaxy. Since the l.o.s. velocity field itself is used to determine these parameters, it is clear that this can influence the resulting harmonic terms. FvGdZ showed that this fitting of the ring parameters from the l.o.s velocity field will affect the expansion given in equation (2) due to a possible difference between the best fitting parameters (i and Γ) and the true parameters. It can be shown that only for $m = 2$ there will be first order differences between the best fitting and true internal parameters, whereas for $m \neq 2$, equation (2) predicts the correct form of the l.o.s. velocity field to second order. In the $m = 2$ case, a misfit of the kinematic centre will result in additional c_0, s_2 and c_2 terms in the harmonic expansion and misfitting of the inclination or position angle will affect the c_1, s_1 and c_3, s_3 terms.

In the case of a globally elongated potential, as caused by for instance a triaxial halo, we have $m = 2$, $\Omega_{2,p} \approx 0$ and $\varphi_2(R) \sim$ const. Note that here we are in the $m = 2$ case, where the best fitting i and Γ are not equal to the true i and Γ. Assuming a flat rotation curve, one finds that after a tilted-ring fit the l.o.s. velocity field has the following form (as derived earlier by FvGdZ):

$$v_{los} = \hat{c}_1 \cos\hat{\psi} + \hat{s}_1 \sin\hat{\psi} + \hat{c}_3 \cos 3\hat{\psi} + \hat{s}_3 \sin 3\hat{\psi}, \qquad (3)$$

with

$$\hat{c}_1 = v_c \sin i (1 - \tfrac{1}{2}\epsilon_v \cos 2\phi_{obs}),$$

3

$$\hat{s}_1 = v_c \sin i \left[1 - \frac{(3q^2 + 1)^2}{(3q^2 + 1)^2 + (1 - q^2)^2} \right] \epsilon_R \sin 2\phi_{obs},$$

$$\hat{c}_3 = 0, \tag{4}$$

$$\hat{s}_3 = v_c \sin i \left[-\frac{(1 - q^2)(3q^2 + 1)}{(3q^2 + 1)^2 + (1 - q^2)^2} \right] \epsilon_R \sin 2\phi_{obs},$$

where $q \equiv \cos i$, $\hat{\psi}$ is the angle in the plane of the ring ($\hat{\psi}$ is zero on the apparent major axis of the ring), ϵ_R is equal to the elongation of the potential and $\epsilon_v = 2\epsilon_R$. We see that from the $\hat{s}_1$ and $\hat{s}_3$ terms we are able to derive $\epsilon_R \sin(2\phi_{obs})$, the quantity that I will try to measure. Unfortunately, one cannot determine ϕ_{obs} separately, so the combination of viewing angle and ellipticity is all one can determine for an individual galaxy. Global ellipticity will create s_1 and s_3 terms that are *constant* with radius (and thus $\epsilon_R \sin(2\phi_{obs})$ will be constant as a function of radius as well), whereas spiral-like perturbances will cause s_1 and s_3 terms that change sign as a function of radius and $\epsilon_R \sin(2\phi_{obs})$ will wiggle. Therefore, I will interpret an average value of $\epsilon_R \sin(2\phi_{obs})$ that is offset from zero as due to ellipticity of the disk.

Strong warping will invalidate the approach discussed above.

3. Some example velocity fields

In order to clarify the equations presented in section 2, we present a number of example potential perturbations and corresponding residual velocity fields in figure [1]. The harmonic terms of the different potential perturbations range from $m = 1$ to $m = 4$. For the phase of the fields, $\varphi_m(R)$, we chose a logarithmic spiral. The amplitude of the perturbation has been taken constant throughout the field. The l.o.s. velocity fields are then created using equation (2) (these are not shown). A tilted-ring fit was then made to these l.o.s. velocity fields and subsequently the harmonic fit was made, revealing the two harmonic components that were hidden in them.

In figure [1] we see from left to right

1. The m term potential perturbation.

2. The residual velocity field (velocity field minus fitted circular velocity) caused by this potential perturbation (i.e. the $m - 1$ plus $m + 1$ terms together).

3. The $m + 1$ component of the residual field.

We see that indeed an m term in the density causes $m - 1$ and $m + 1$ terms in the kinematics of the gas. In these examples, the $m - 1$ term is dominant.

Equation (2) predicts that the c_3 term should be fitted to zero by the tilted-ring fit in the case of a $m = 2$ perturbation in the potential. Thus, in the $m + 1$ component of the residual field, no spiral-like structure should be visible any more. In figure [1], we see that this is indeed the case. Instead of spiral structure, we see radially alternating positive and negative contributions, caused solely by the $s_3(R)$ term. If the potential would have contained a global
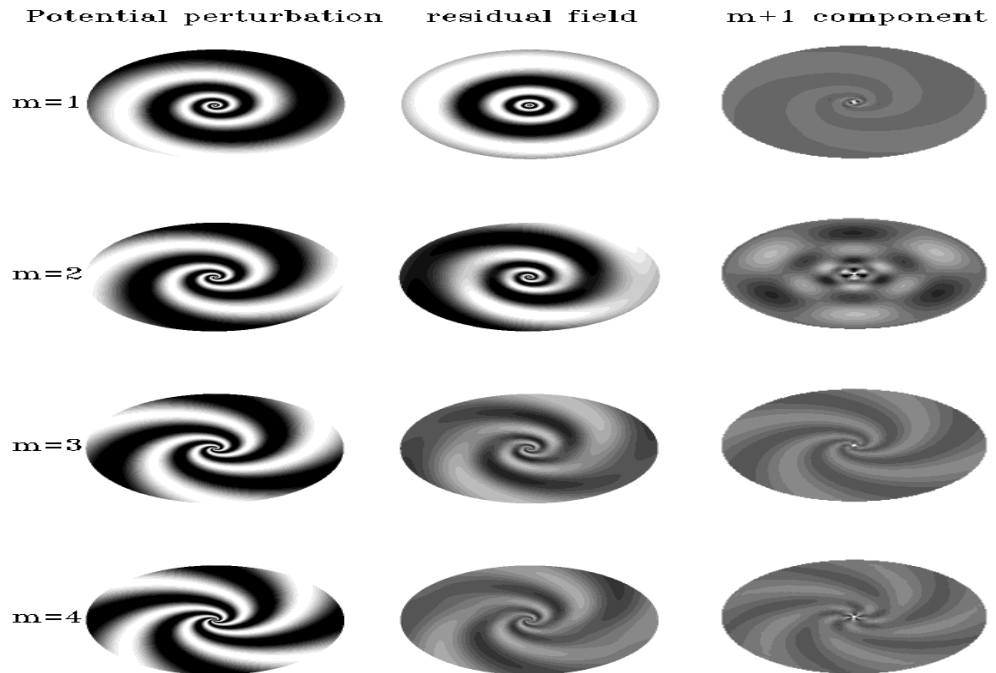
4

Potential perturbation   residual field   m+1 component

Figure 1.   Potential perturbations and velocity fields. We created a potential with a perturbation as given in equation (1) with a single m (ranging from 1 to 4, shown in column 1). Subsequently we calculated the velocity field corresponding to this potential using equation (2) and made a tilted-ring fit to this field. This gave us a residual velocity field (column 2). This residual field is dominated by the $m - 1$ component. A harmonic fit to the velocity field revealed that the residual field contained the $m + 1$ term as well (column 3).

intrinsic ellipticity, $m = 2, \varphi_2(R) = $ const, the s_1 and s_3 terms caused by this elongation would have been constant as a function of radius. Therefore, the measured s_3 would have been constant and non-zero as well and no radially alternating pattern for s_3 would have been visible in this plot.

Since in the fitting procedure the centre was kept fixed, we also see a two-armed spiral in the $m + 1$ residual field of the $m = 1$ potential perturbation. If we would have taken the centre as a free parameter in the fit, it would have drifted in such a way as to make the c_2 and s_2 terms disappear.

4.   Two test cases: NGC 2403 and NGC 3198

4.1.   Data description

NGC 2403 is a nearby (3.25 Mpc; Begeman, 1987) Sc(s)III galaxy (Sandage & Tammann, 1981). It has been observed with the WSRT, 4×12 hours (Sicking, 1996). The data have been smoothed to a circular beam of 13 arcseconds. The second relatively nearby (9.4 Mpc; Begeman, 1987) spiral galaxy we will examine
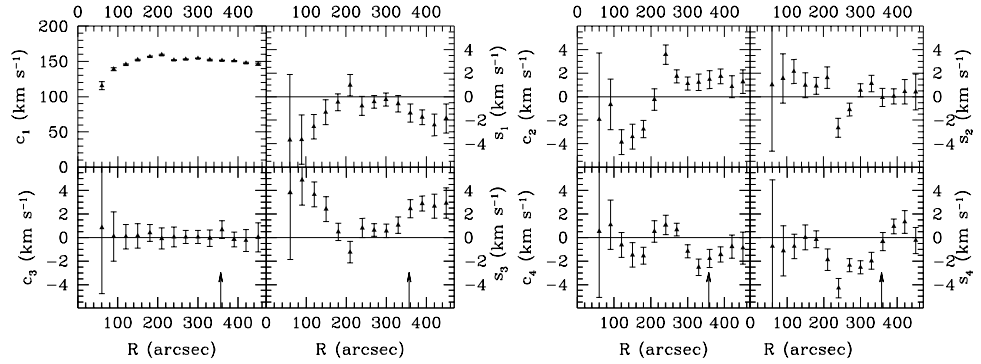
5

Figure 2.   Harmonic decomposition of the velocity field of NGC 3198. Only the first four terms of the expansion are shown, since higher order terms have low amplitudes. The c_1 term gives the circular velocity, i.e. the rotation curve. From the s_1 and s_3 terms $\epsilon_R(R)\sin(2\phi_{obs})$ will be measured. The c_2, s_2 terms are zero if the kinematic centre of a ring is left free in the fit. Since the same (fixed) centre is taken for all rings here, the c_2, s_2 terms vary. Especially in the inner parts the c_2 term is relatively large, indicating that NGC 3198 might be somewhat lopsided. The c_3 term is zero if the inclination is fitted correctly (equation 4), which is obviously the case here. There is also some power in the c_4, s_4 modes. This may be caused by some three- or five-armed spiral structure (see figure 1). Visual inspection of the HI surface density map shows a three-fold spiral-like structure. The arrows denote the Holmberg radius.
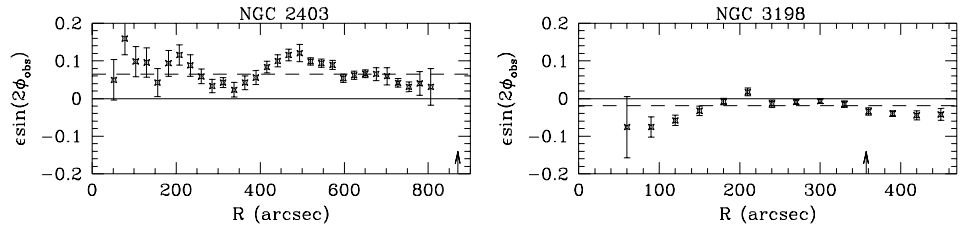

Figure 3. $\epsilon_R(R)\sin(2\phi_{obs})$ as a function of radius. The effect in NGC 2403 may be caused by spiral arms. The average value is used as an upper limit to the halo ellipticity. The measurement for NGC 3198 is relatively straight within errors and very low. The dotted line is the average value of $\epsilon_R(R)\sin(2\phi_{obs})$, the arrow denotes the Holmberg radius.

is the Sc(rs)I-II (Sandage & Tammann, 1981) galaxy NGC 3198. This galaxy was observed by Sicking (1996) with the WSRT, also for 4×12 hours. The observations have a circular beam with FWHM of 18 arcsec. Both galaxies are well suited for our type of analysis: they have large extents on the sky (Holmberg dimensions: NGC 2403: $29'.0 \times 15'.0$ and NGC 3198: $11'.9 \times 4'.9$), have a favourable inclination (NGC 2403: $i \approx 62^o$, NGC 3198: $i \approx 71^o$), the data have high signal/noise, the beams are small and both galaxies show no obvious warp. The residual maps of the galaxies show only small (typically < 10 km s^{-1}) residuals, but they appear to contain systemic structures.

4.2. Measuring the elongation

The first step in our procedure is to fit concentric tilted–rings to the l.o.s. velocity fields of these galaxies. The width of each ring is taken to be about twice the beam size, to be sure that all the individual rings are independent. Table [1] lists the radially averaged ring parameters found by the tilted-ring fit.

Parameter	NGC 2403	NGC 3198
position angle	$124^\circ.1 \pm 0^\circ.09$	$215^\circ.93 \pm 0^\circ.13$
inclination	$61^\circ.5 \pm 0^\circ.20$	$70^\circ.6 \pm 0^\circ.21$
systemic velocity	133.3 ± 0.10 km s^{-1}	660.1 ± 0.16 km s^{-1}
$\epsilon_R \sin(2\phi_{obs})$	0.064 ± 0.003	-0.019 ± 0.003

Table 1. Radially averaged ring parameters for NGC 2403 and NGC 3198

After the tilted–ring fit a harmonic fit was made to the velocity fields along each individual ring. Harmonic terms were measured up to ninth order. In figure [2], the result for the first four harmonics of NGC 3198 are shown as an example. The c_3 term is zero everywhere in both galaxies, indicating that the inclination is correctly fitted for all rings. Furthermore, we find that in both galaxies harmonics c_n, s_n with $n > 5$ are consistent with zero. In the lower harmonics, clear systematic trends (as a function of radius) are visible. Using $s_1(R)$ and $s_3(R)$, we are able to measure $\epsilon_R(R) \sin(2\phi_{obs})$. The results of these measurements are given in figure [3], where we see that $\epsilon_R(R) \sin(2\phi_{obs})$ strongly wiggles as a function of radius for NGC 2403, whereas for NGC 3198 it is fairly constant within errors. Furthermore, note that $\epsilon_R(R) \sin(2\phi_{obs}) > 0$ for NGC 2403 at all radii. This indicates that, although spiral arms are present that cause the wiggling, there may also be a global elongation present, lifting $\epsilon_R(R) \sin(2\phi_{obs})$ from an average of 0 to an average of 0.064 ± 0.003. For NGC 3198 the average value of $\epsilon_R \sin(2\phi_{obs})$ is very low: -0.019 ± 0.003.

Since the effect of ellipticity and spiral arms cannot be separated unambiguously, these measurements suggest that spiral galaxies are close to axisymmetric. But more galaxies are needed in order to quantify this result (Schoenmakers *et al.*, in preparation).

7

References

Begeman K., PhD-thesis, University of Groningen, 1987

Binney J., 1978, MNRAS, 183, 779

Binney J., Tremaine S., Galactic Dynamics , 1987, Princeton University Press

Binney J., de Vaucouleurs G., 1981, MNRAS, 194, 679

Canzian B., 1993, ApJ, 414, 487

Dubinski J., 1994, ApJ, 431, 617

Dubinski J., Carlberg R.G., 1991, ApJ, 378, 496

Fasano G., Amico P., Bertola F., Vio R., Zeilinger W.W., 1992, MNRAS, 262, 109

Franx M., de Zeeuw P.T., 1992, ApJ, 392, L47

Franx M., van Gorkom J.M., de Zeeuw P.T., 1994, ApJ, 436, 642 (FvGdZ)

Gradshteyn I.S., Ryzhik I.M., 1965, Table of Integrals, Series and Products, New York: Academic Press

Holmberg E., 1958, Medd. Lund Obs. Ser. II, 136

Katz N., Gunn J.E., 1991, ApJ, 377, 365

Kuijken K., Tremaine S., 1994, ApJ, 178, 421

Lambas D.G., Maddox S.J., Loveday J., 1992, MNRAS, 258, 404

van der Marel R., 1991, MNRAS, 248, 515

Navarro J.F., Frenk C.S., White S.D.M., 1996, ApJ, 462, 563

Olling R.P., 1995a, AJ, 110, 591

Olling R.P., 1995b, BAAS, 187, 48.05

Rix H-W., Zaritsky D., 1995, ApJ, 447, 82

Sackett P.D., Rix H-W., Jarvis B.J., Freeman K.C., 1994, ApJ, 436, 629

Sackett P.D., Sparke L.S., 1990, ApJ, 361, 408

Sandage A., Tammann G.A., 1981, Revised Shapley-Ames Catalogue of Bright Galaxies (Carnegie Inst. of Washington Pub. No. 635)

Schoenmakers R.H.M., Franx M., de Zeeuw P.T., in prep.

Sicking F.J., PhD-thesis, University of Groningen, 1997

Teuben P., 1991, in Warped Disks and Inclined Rings around Galaxies, (eds. S. Casertano, P.Sackett, F. Briggs), Cambridge Univ. Press.

Tohline J.E., Simonson G.F., Caldwell N., 1982, ApJ, 252, 92

Whitmore B.C., McElroy D., Schweizer F., 1987, ApJ, 314, 439